ACS Photonics

pubs.acs.org/journal/apchd5

Article

High-Resolution Multicolor Patterning of InP Quantum Dot Films by Atomic Layer Deposition of ZnO

Joon Yup Lee, Eun A Kim, Yeongho Choi, Jisu Han, Donghyo Hahm, Doyoon Shin, Wan Ki Bae, Jaehoon Lim, and Seong-Yong Cho*

Cite This: *ACS Photonics* 2023, 10, 2598−2607

Read Online

ACCESS | Metrics & More | Article Recommendations | Supporting Information

ABSTRACT: This paper presents the high-resolution (>2000 PPI) multicolor patterning of InP quantum dot films using a conventional photolithography process with a positive photoresist (PR). The solvent resistance of the quantum dot (QD) film is achieved by depositing an ultrathin ZnO layer through atomic layer deposition. This is different from previous studies, which lack high-resolution patterning or compatibility with indium phosphide (InP) QDs owing to chemical weaknesses. By employing a positive PR with a photoacid generator, the side-by-side patterning process yields multicolor patterns of red- and green-colored InP-based QDs. Additionally, the stacking of each color QD film is achieved. The patterning process can be used to fabricate QD light-emitting diode devices without degrading their performance. This process can be used not only for thin (<100 nm) QD films, which are used in QD-LED devices, but also for thick (>1 μm) QD films, which can be used in the color-conversion layer with a backlight.

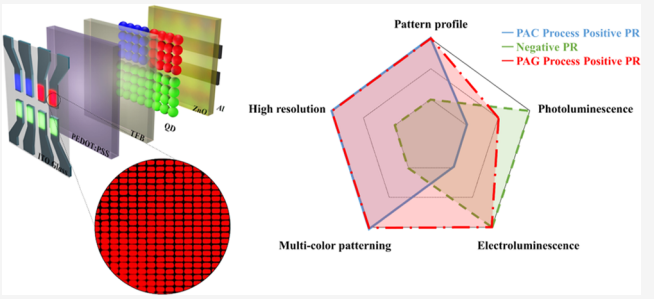

KEYWORDS: *InP quantum dots, patterning, photolithography, atomic layer deposition, thick QD patterning, photoacid generator*

INTRODUCTION

Semiconductor nanocrystals and colloidal quantum dots (QDs) are potential emissive display materials owing to their high color purity, large-scale synthesis, and solution processability.[1−3] Typically, QDs are incorporated into multilayer thin-film devices to fabricate functional devices, such as light-emitting diodes.[4−10] Although Cd-based QDs have frequently been used in QD electroluminescence (EL) devices, the Restriction of Hazardous Substances Directive strictly regulates the use of toxic elements. Therefore, the synthesis of Cd-free QDs has been investigated extensively.[11−13] Currently, indium phosphide (InP) is the most widely used material for heavy-metal-free QD synthesis, and the performance of InP-based QD EL devices has improved significantly, up to higher than 20% of the external quantum efficiency (EQE), by optimizing both the QD synthesis and the device architecture.[13] Both red and green QD emissions with almost unity photoluminescence quantum yield (PLQY) in InP-based QDs have been achieved by synthetic parameter control and state-of-the-art core and shell design. Additionally, blue emission in eco-friendly QD materials has also been attempted by searching for heavy-metal-free post-InP QDs, such as InGaP and ZnSeTe alloys.[12,14−16]

In addition to QD EL applications and color-conversion uses for QDs, the patterning of QD pixels is required.[17] The inkjet printing method is currently used for QD pixel formation; however, high-resolution patterning for augmented and virtual reality (AR/VR) applications (>1000 PPI) is limited owing to the physical size of the ink droplet.[18−20] Additionally, nozzle clogging and the coffee ring effect are fundamental limitations. Although transfer printing and electrohydrodynamic jet printing can provide relatively high-resolution QD patterns,[21−24] optical lithography is an ideal method for patterning high-resolution QD patterns,[21−24] considering that this technique is well established in the semiconductor industry.[25−29] Typical photopatterning of QD films involves the use of photosensitive and cross-linkable ligands or additives to provide solvent resistance to the QD areas exposed to light.[30,31] However, QD and photosensitive organic molecule mixtures inevitably reduce the color-conversion efficiency of QD color filters and charge injection in light-emitting diode (LED) devices. Additionally, the typical method is limited to a certain QD film thickness, owing to the limited penetration depth of UV light in the QD film.[32]

Depositing ultrathin ZnO on the QD surface or cross-linking the QD film surface is an effective approach to providing solvent resistance to the QD film.[33] In our previous studies,

Received: March 10, 2023
Published: June 22, 2023

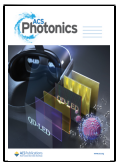

https://doi.org/10.1021/acsphotonics.3c00332
ACS Photonics 2023, 10, 2598−2607

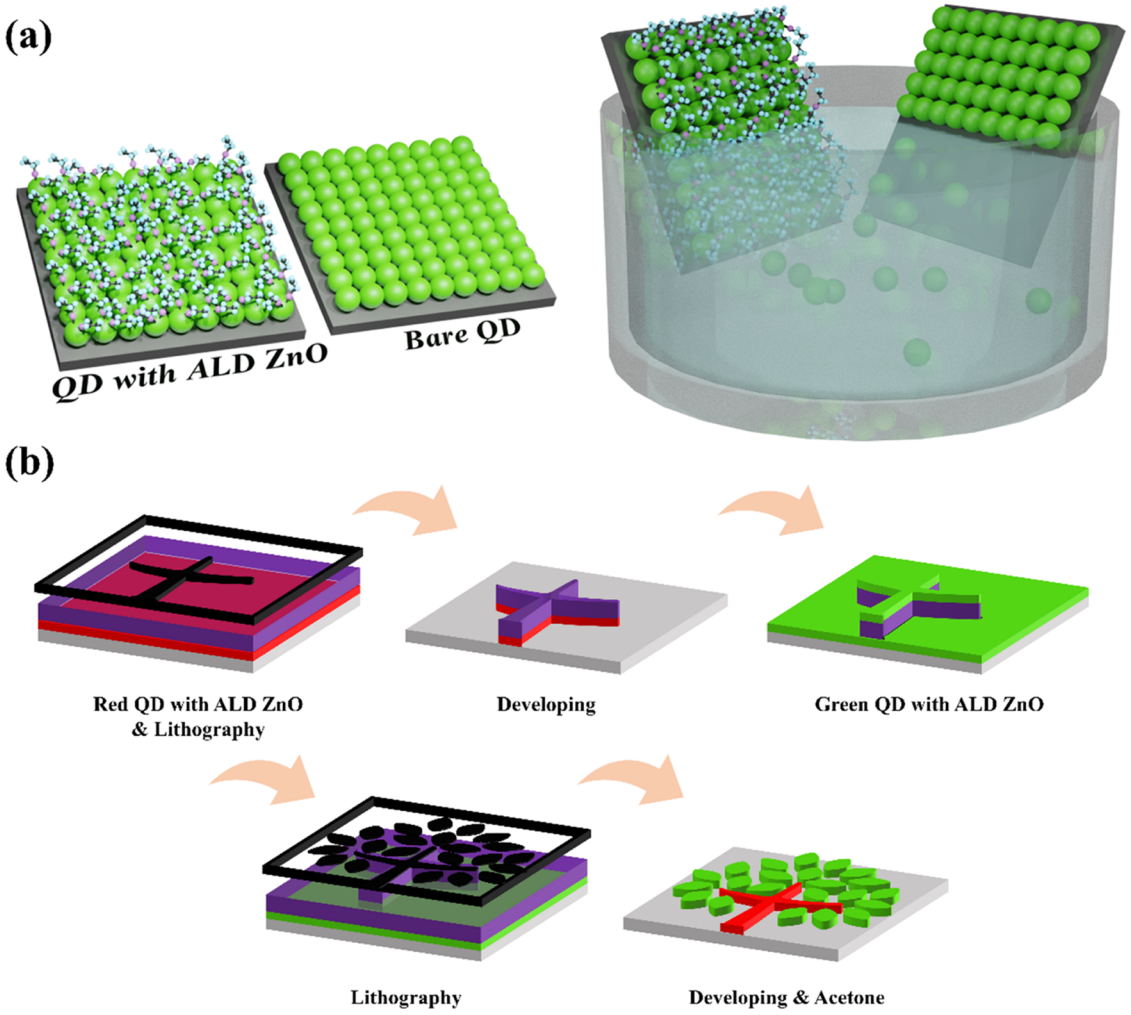

Figure 1. Schematics of the surface cross-linking of the InP QD film and photolithography-based patterning process in this study: (a) QD film with ALD ZnO and a bare QD film on substrates are dipped into the solvent and (b) the multicolor (red and green, respectively) QD film patterning process with repeated steps of photolithography processes.

photolithography-based high-resolution patterning of QD films was achieved by directly coating a photoresist (PR).[27,29] The Cd-based QD film was easily patterned by conventional PR coating, but the InP-based QD film was severely damaged during PR coating owing to the chemical weakness of the InP-based QD. Despite the solvent resistance of the QD film by the deposition of ultrathin ZnO films through atomic layer deposition (ALD), significant photoluminescence (PL) quenching was observed during the PR coating and subsequent photolithography process.[27,34] The negative-type PR successfully suppressed the PL quenching of the InP QD film by removing the sulfonic group; however, multicolor QD film patterning was not achieved owing to the hardening of the negative PR.[29] In this study, a photoacid generator (PAG)-type PR was employed to fabricate high-resolution multicolor InP-based QD films with patterns. The PR did not significantly degrade the PL intensity of the InP-based QD film, owing to the absence of a chemically strong group, and a patterned QD EL device was fabricated using the InP-based QD. After the patterning process, the InP-based QD EL device did not exhibit any noticeable performance degradation compared with the QD EL device without the patterning process.

RESULTS AND DISCUSSION

Figure 1 shows the schematics of the QD surface cross-linking and photolithography-based QD film patterning process through the ALD of ZnO in this study. Figure 1a shows the QD films with and without ALD ZnO surface passivation, which exhibit different solvent resistance properties. Typical aliphatic ligands, such as oleic acid and oleylamine, are not shown in the schematic, but the formation of ALD ZnO is adequately addressed. Similar to our previous studies,[27,29,34] the QD films subjected to ALD treatment exhibited improved device performance and significantly improved solvent resistance during the photolithography process. The QD solvent-dipping image in Figure 1a shows the different solvent resistances in the QD films with and without ALD ZnO treatment. Even if the ALD-treated QD film is dipped into toluene, which is the mother solvent of the QD, the film does not dissolve. In contrast, the bare QD film was easily dissolved by toluene. Typically, the ligand attached to the shell facilitates dispersion in a solvent such that when this phenomenon occurs, a reaction occurs between the shell surface and the ligand during the ALD process of ZnO. This is attributed to the existence of diethyl zinc (DEZ) precursors around the ligand, which causes cross-linking between the ligands. Another reason could be the ligand exchange between the

https://doi.org/10.1021/acsphotonics.3c00332
ACS Photonics 2023, 10, 2598−2607

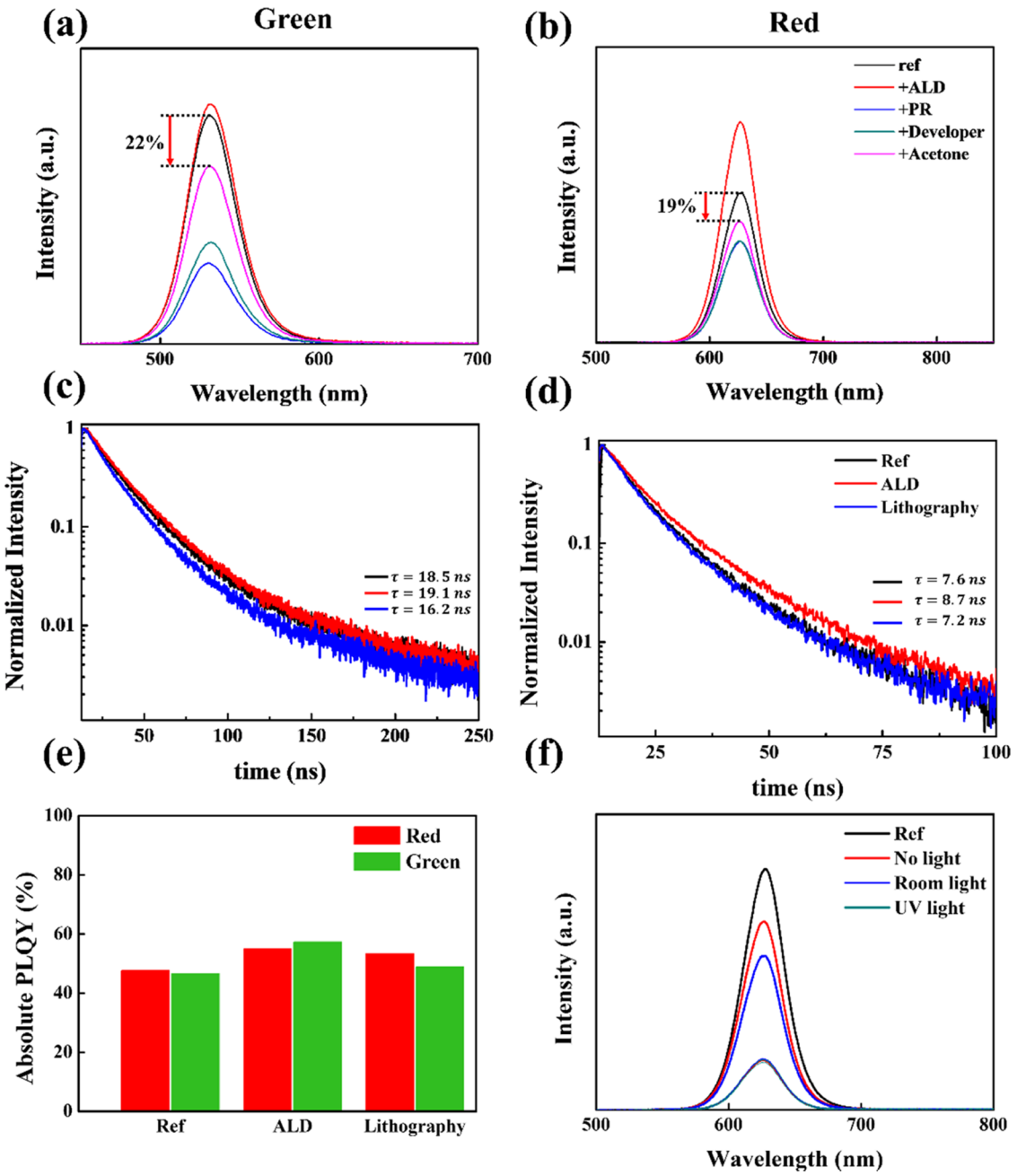

Figure 2. Relative PL intensities of (a) green- and (b) red-colored InP-based QD films after depositing ALD ZnO, spin-coating the PR, developing, and stripping the PR; time-resolved PL decay curves of (c) green- and (d) red-colored InP-based QD films after the ALD ZnO deposition and photolithography process; (e) absolute PLQY of red and green InP-based QD films after the ALD ZnO deposition and lithography process; and (f) relative PL intensities of the InP-based QD film coated by a positive PR (AZ 12XT) under room and UV light.

pre-existing organic ligands and the DEZ. Because the ligands detach from the shell during the thermal ALD process, Zn, which is a part of DEZ, is attached to the vacancy, and one of the ethyl groups becomes a QD ligand. Consequently, owing to solvent resistance, the QD film can be patterned using conventional photolithography, as shown in Figure 1b. The PR was coated onto the QD film, which was treated using the ALD process of ZnO, followed by UV light exposure and development. This photolithography process does not require an etching process because a developer (tetramethyl ammonium hydroxide (TMAH) solution) can dissolve the QD film while developing the PR. Typically, ZnO is dissolved by acid and base solvents such that the developer can strip the QD film, which is treated by the ALD of ZnO. After the development process, a QD film of another color was deposited onto the sample, and the patterning process was completed after repeating the same procedure. Thus, a multicolor pixelated display was easily fabricated.

For the use of InP-based QDs with red and green emission colors, Figure 2a,b shows the PL intensities of the green and red InP QD films during each step of the photolithography process. The ALD-treated QD film exhibits higher intensity compared with the bare QD film, possibly owing to surface defect passivation, which is in good agreement with the findings of our previous study.[34] After PR coating, the PL intensity decreased owing to the absorption of the UV

https://doi.org/10.1021/acsphotonics.3c00332
ACS Photonics 2023, 10, 2598−2607

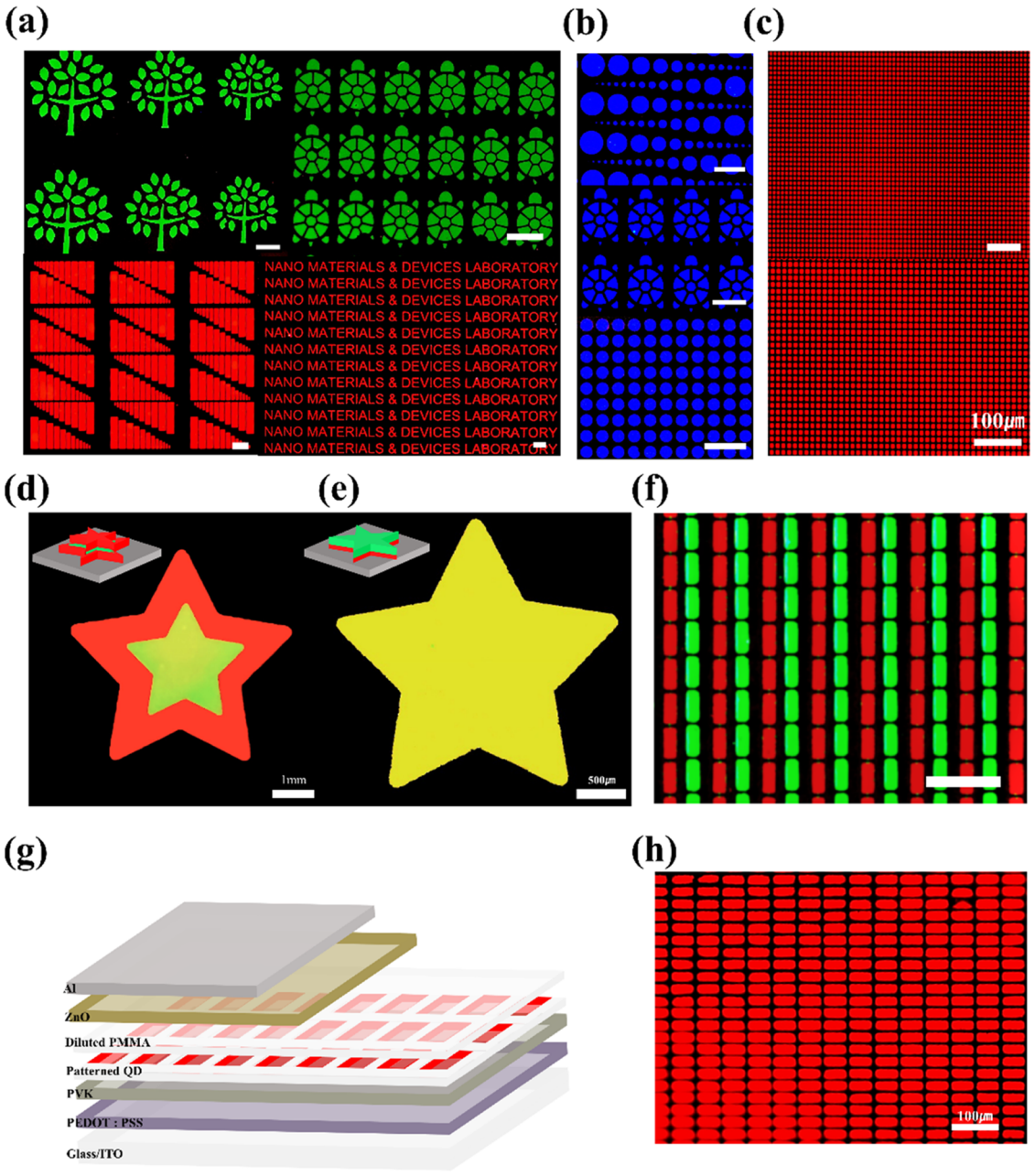

Figure 3. (a) Various shapes of (a) red- and green-colored InP-based QD film patterns and (b) ZnSeTe-based QD film patterns; (c) high-resolution red InP QD patterns over 2000 PPI (7 μm width, 9 μm heigh); (d, e) stacked star-shaped patterns of red and green InP-based QDs exhibiting yellow color in the merged area; (f) high-resolution (800 PPI) pixel arrays of red and green InP-based QD patterns obtained by fluorescence microscopy (16 μm width, 40 μm height); and (g) schematic of the QD-LED device for the patterned EL image in panel (h).

excitation source by the thick photoresist itself. Additionally, the photoluminescence of the QD patterns was the same as that after PR coating, as indicated by the blue line, because the samples remained under the PR after development. However, when the samples were dipped in acetone to strip the PR, the photoluminescence increased in both the red and green InP QDs. Consequently, in the case of the green InP-based QD, the PL decreased by approximately 22%, whereas in the case of the red InP-based QD, the PL decreased by 19%. The same trends are also observed in the time-resolved spectra in Figure 2c,d and do not exhibit a significant decay path after the lithography process. The absolute PLQY of the InP QD film after the deposition of ALD ZnO was slightly higher, and no PLQY reduction was observed after the lithography process, as shown in Figure 2e. The reason for the slight reduction in PL is typically related to the materials used in the photolithography process, and it is likely that the main reason is related to the PR instead of the developer or acetone. The application of a positive PR (AZ GXR 601), which includes DNQ (a photoactive compound (PAC) in a positive PR), to photolithography[27] results in significant PL reduction. In contrast, in a previous study,[29] a negative PR (DNR L300 40) did not exhibit a significant reduction in the QD PL. In this study, the positive PR used in the QD patterning process did not include PAC, and direct contact with this PR did not damage the QD films. Instead, the positive PR used in this study (AZ 12XT) contains a photoacid generator (PAG) that generates a large amount of acid when exposed to light. Figure 2f shows the

https://doi.org/10.1021/acsphotonics.3c00332
ACS Photonics 2023, 10, 2598−2607

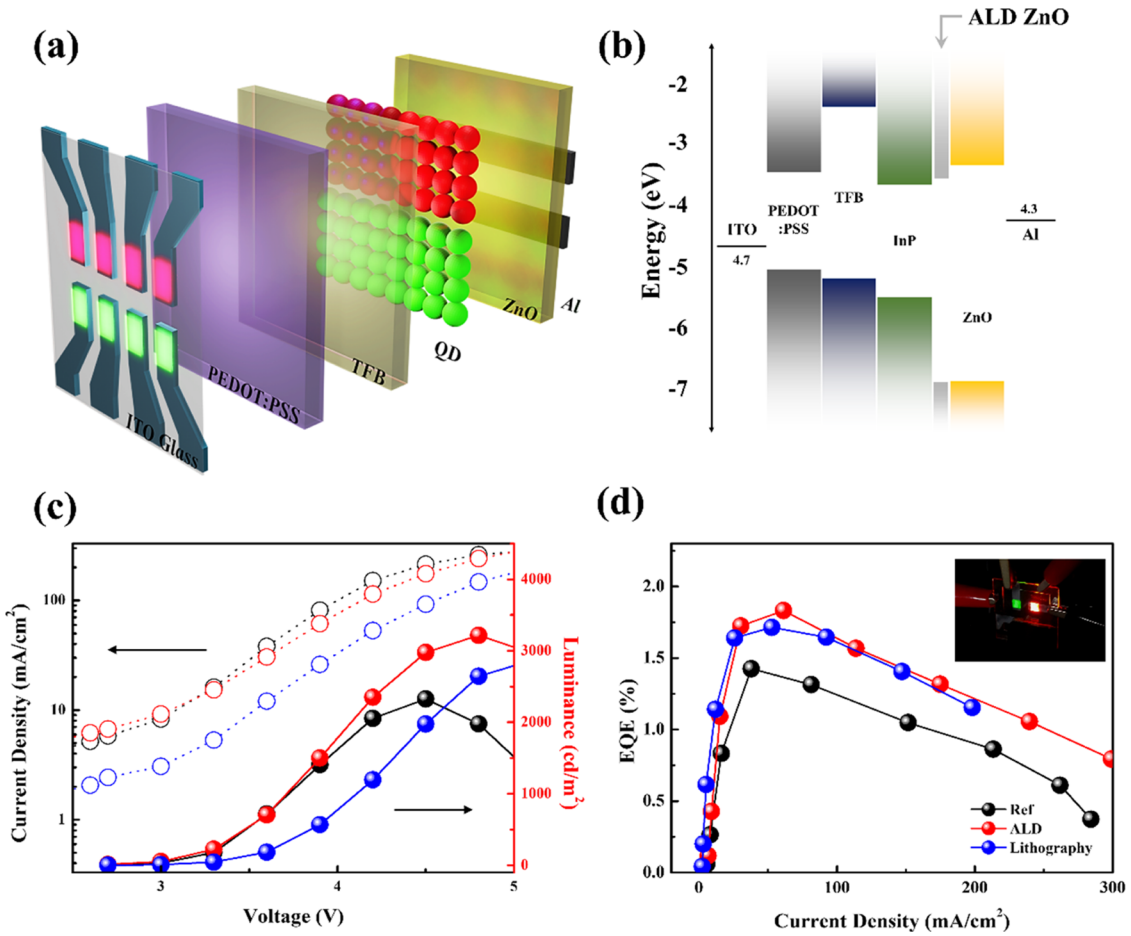

Figure 4. (a) Schematic of the InP-based QD-LED with the photolithography patterning process for EML pixel formation; (b) expected electronic band diagram of the InP-based QD-LED in this study; (c) current density and luminance of the red InP-based QD-LED; and (d) EQE of the InP-based QD-LED reference device after the ALD ZnO deposition and lithography process.

relative PL intensities of the InP QD films after PR coating and exposure to UV and room light. A significant amount of PL was quenched; however, these areas were removed during the patterning process owing to the working principle of the positive PR. The remaining area after the patterning process was not exposed to UV light. In contrast, the PAC-type PR resulted in permanent damage to the QD film when coated, as shown in Figure S1. Additionally, during the lithography process, no obvious changes in the PL peak or broadening were observed, indicating that the QDs were not aggregated (Figure S2). The PL intensities of the Cd-based QD films after patterning are shown in Figure S3.

The QD film patterning process was the same as that of conventional photolithography, except that an additional etching process was not required, as shown in Figure S4 and discussed in the experimental section. Figure 3a shows the various shapes and patterns of the red and green colors of the InP-based QD, which is a promising eco-friendly emitter material; however, blue emissions are not feasible owing to its extremely small exciton Bohr radius.[11] Therefore, to form blue QD patterns, a ZnSeTe-based QD film was used for patterning in this study, as shown in Figure 3b. The relative PL intensities during each step of photolithography were measured for the ZnSeTe-based QD film. Because of the extremely low stability of the ZnSeTe QD film in air, aliphatic ligands were exchanged with thiol ligands in the PL study, as shown in Figure S5. For practical pixelated display applications, both high-resolution patterning and multicolor pixel formation are required. In our previous work on a positive PR,[27,29] the PR coating severely deteriorated the PL intensity of the InP-based QD film; therefore, a negative PR was introduced to minimize the PL quenching behavior, but multicolor patterning was not achieved owing to the hardening of the PR, and the negative sidewall formed pattern shrinkage during the patterning process. The positive PR used in this study does not contain a PAC that degrades the QD film and is compatible with high-resolution patterning (>2000 PPI), as shown in Figure 3c. Higher resolution can be achieved by optimizing the process parameters, such as the baking temperature of the PR and the light-exposure dose during the lithography process. Direct stacking of the red and green InP QD films is also possible, as shown in Figure 3d,e. The red QD film coated on top of the prepatterned star-shaped green QD film exhibited a larger red QD pattern with a star shape and yellow star in the center, as shown in Figure 3d. A schematic of a bird's-eye view of the structure is shown in the inset of Figure 3d. Figure 3e shows the exact overlap of the two-star shapes. It can be seen that a yellow pattern was achieved. A schematic of a bird's-eye view of the structure is shown in the inset of Figure 3e. Red and green InP-based QD films were also successfully fabricated using side-by-side patterning (800 PPI), as shown in Figure 3f. The details of the side-by-side multicolor patterning are shown in Figure S4. To test the patterning process in an EL device, a pixel define layer (PDL) is required. For example, in a typical

https://doi.org/10.1021/acsphotonics.3c00332
ACS Photonics 2023, 10, 2598−2607

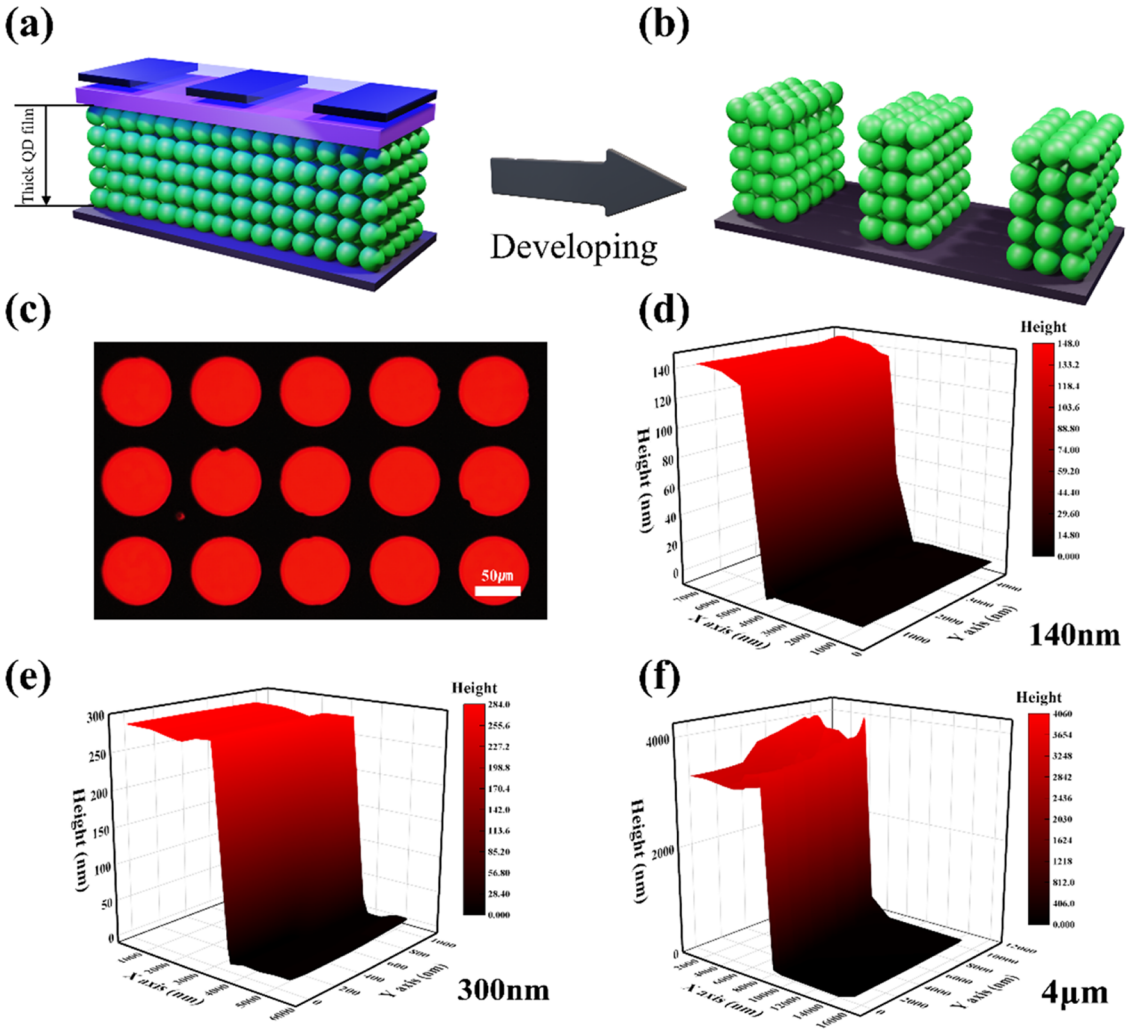

Figure 5. (a) Thick QD film passivated by ALD ZnO and a patterned PR on top; (b) thick QD pattern after the developing process; and (c) top-view fluorescence microscopy image of thick (300 nm) patterns and depth profile of (d) 140, (e) 300 nm, and (f) 4-μm thick QD patterns achieved by the 3D optical surface profiler.

inkjet patterning process of a QD film, a PDL is formed prior to the fabrication of a QD pixel using ink. Without the PDL, direct contact between the HTL and ETL forms a lower resistance in the area without QD patterns (current leakage path), and eventually, the QD pixel will not emit light. To prevent this issue, Hu et al. used diluted poly(methyl methacrylate) (PMMA) to suppress the current leakage, as shown in Figure 3g.[35] By adopting the same strategy, a patterned EL image was successfully obtained after depositing a thin PMMA (<3 nm) layer, as shown in Figure 3h, and the image was the same as the PL image. The EL image in Figure 3h is stable, but the same EL pattern without PMMA passivation does not work because of the large leakage current in the area without QD patterns.

Figure 4a shows the structure of the QD-LED device using InP-based QD after the patterning process. The pixel size is larger than the size of electrode overlaps (6 mm^2) to measure device efficiency. Before the photolithography-based QD patterning process, indium tin oxide (ITO), hole injection and hole transport layers (HIL and HTL), and QD films were prepared; the patterning process was performed to fabricate pixelated QD-LED devices. The deposition of ZnO and Al cathodes completes the fabrication of QD-LED devices. A band diagram of the QD-LED device is shown in Figure 4b with ALD ZnO between the InP and ZnO ETL. The energy band of ALD ZnO and ZnO ETL were measured using ultraviolet photoelectron spectroscopy (UPS) analysis, as shown in Figure S6. Similar to the results obtained in a previous study,[27,34] the interlayer of the ZnO film achieved improved performance compared with a device lacking an interlayer. Figure 4c shows the current density and luminance of the InP-based QD-LED with the reference structure and after the ALD ZnO deposition and lithography process. Notably, the current density of the ALD ZnO-deposited InP QD-LED was lower than that of the reference QD-LED device. Additionally, the luminance increased after the deposition of the ALD ZnO interlayers. Although the luminance decreased after the patterning process, the EQE of the QD-LED device after patterning had a higher value owing to the suppressed current density, as shown in Figure 4c,d. The inset in Figure 4d shows the successful fabrication of red- and green-colored QD pixels in a single substrate by the patterning process in this work.

A striking advantage of the direct PR coating enabled by the ALD-based surface cross-linking of the QD films is that it enables the simple fabrication of thick QD film patterns of up

https://doi.org/10.1021/acsphotonics.3c00332
ACS Photonics 2023, 10, 2598−2607

to a few microns. For electroluminescent devices, several monolayers of the QD pattern are sufficient, but thicker QD films inhibit charge transport. However, for the down-conversion of a backlight unit, such as a liquid crystal display, OLED, or micro-LEDs, a relatively thick fluorescence material is required owing to the limited absorption of the backlight at a certain thickness. The thin QD film passes the backlight without converting it to the desired color. Although typical photolithographic patterning processes with photosensitive ligands or additives in QD solutions can effectively fabricate QD pattern films with thicknesses of tens of nanometers, they cannot be applied to the fabrication of thicker films of up to microns. This is because most of the light source is absorbed by QDs at the surface considering the large amount of absorbance at the UV regime. Li et al.[32] demonstrated thick QD film patterning using near-infrared lasers; however, their process was not compatible with projection-type lithography with a photomask, which means that mass production is not possible. The proposed QD film patterning method is based on surface cross-linking and direct PR coating owing to surface passivation via ALD ZnO. Therefore, in addition to thin QD films for QD EL device applications, thick QD films for QD color-conversion devices can be patterned using this method. Figure 5a shows a schematic of a thick QD film with ALD ZnO passivation and a patterned PR. Through the simultaneous development of the PR and etching of the QD film, micrometer-sized patterns can be easily formed, as shown in Figure 5b. Figure 5c shows a fluorescence microscopy image of the dot patterns with various QD film thicknesses, and Figure 5c–e shows the depth profiles of the QD films with various initial thicknesses. As can be clearly seen, QD films with various thicknesses (140 nm, 300 nm, and 4 μm) can be patterned, which was not possible in previous studies, using the light-sensitive cross-linking method. The surface nonuniformity in the 4-μm QD film was caused by the dip-coating process because typical spin-casting cannot form a relatively thick QD film.

Figure S7 shows a comparison of the direct photoresist coating on the QD and lithography process in terms of several aspects. All lithography-based QD patterning is possible by depositing ultrathin ALD ZnO and direct spin-casting the PR on top of the QD film. First, the PAC process with a positive PR (GX 601, Merck) provides high-resolution and multicolor QD patterns by side-by-side patterning, but the QD film is damaged during PR coating due to the presence of a strong acid sulfonic group in PAC, and the process is not compatible with Cd-free QDs such as InP.[27] QD patterning by negative PR is much softer with no PL quenching and is compatible with InP-based QD films; however, the hardening of PR during the lithography process makes it difficult to be used for high-resolution patterning. In addition, multicolor QD film formation is not easy because the removal of PR is not possible during repeated steps of lithography.[29] Finally, the PAG process-based positive PR (AZ 12XT in this work, Merck) can provide high-resolution multicolor QD patterns with no significant damage to the InP-based QD film. The damage in the QD film does not result from the PR coating but is induced by UV exposure when the PR with the PAG component is coated.

CONCLUSIONS

In this study, environmentally benign InP-based QD films were successfully patterned by conventional photolithography using a PAG-type positive PR. Furthermore, high-resolution (>2000 PPI) multicolored InP QD film patterns were achieved without significant PL quenching during the lithography process, owing to the absence of PAC, which degrades the QD film simply by forming a coating on top of the QD film and through physical contact, according to our previous study. The QD film area degraded by UV exposure on the PAG in the PR was removed during the lithography process, and the remaining QD film area did not exhibit any noticeable PL degradation. A QD patterning process was used to fabricate the patterned QD-LED device, and the performance of the fabricated QD-LED device did not degrade after the patterning process. Furthermore, the proposed patterning process is not only applicable to thin QD films but also to thick QD films, which can be used for the down-conversion of the backlight in LCD or OLED devices.

METHODS

QD Synthesis. Red- and green-emitting InP/ZnSe/ZnS core/shell (C/S) QDs were prepared as described by Hahm et al.[12,36] Blue-emitting ZnTe/ZnSe C/S QDs were prepared as described by Kim et al.[15] The synthesis of red-emitting CdSe/CdS/CdZnS C/S QDs was carried out through a one-pot procedure, the details of which were described by Borg et al.[37] Green-emitting CdZnSeS/ZnS C/S QDs were synthesized using a one-pot procedure, as described in our previous work.[27,34] Blue-emitting CdZnS/ZnS C/S QDs were prepared as described by Bae et al.[38]

ZnO Nanoparticle Synthesis. ZnO nanoparticles are synthesized by reacting 2.95 g of zinc acetate dihydrate with 1.48 g of potassium hydroxide (KOH).[39] The zinc acetate dihydrate and KOH are added to 125 and 65 mL of anhydrous methanol, respectively, and dissolved with stirring. Once both solutions have reached a temperature of 60 °C, the KOH solution is added dropwise to the zinc acetate dihydrate solution and stirred for 2 h at 60 °C. The resulting solution is allowed to settle for one day. The resulting ZnO nanoparticles were washed thoroughly with methanol three times by centrifuging the solution and then dissolved in butanol at a concentration appropriate for use. To improve the dispersion of the ZnO solution diluted in butanol, 1.6 μL of ethanolamine was added to 1 mL of butanol.[40] The resulting mixture was then filtered through a 0.25 μm PTFE filter to remove impurities from the ZnO solution.

QD Film Patterning. The process of patterning the QD film was similar to that described in a previous report.[29] The QD film was deposited on Si and SiO_2 or a glass substrate, which was cleaned using acetone and isopropyl alcohol (IPA). After QD baking at 180 °C for 30 min to remove the solvent, the substrate was moved into an N_2-filled glove box and was subjected to the ALD process. For the deposition of ZnO on the QD film, DEZ and H_2O were used as the precursor and reactant, respectively. The ALD process was performed for 15 cycles (2 nm) of ZnO. The DEZ and H_2O pulsing times were 0.1 s, and the purging times were 15 s and 50 s, respectively. After the ALD process, a positive PR (AZ 12XT, Merck) was coated on the QD film with ZnO at 3000 rpm for 30 s, and soft baking was performed at 110 °C for 2 min. The film was exposed to UV light after alignment by using an appropriate photomask at 100 mJ/cm^2. After exposure, post-exposure baking was performed at 90 °C for 1 min. The substrate was dipped into a developer (2.38% TMAH solution) and acetone to realize the patterns and etching process simultaneously.

https://doi.org/10.1021/acsphotonics.3c00332
ACS Photonics 2023, 10, 2598−2607

QD-LED Fabrication. The patterned ITO/glass was cleaned several times with acetone, ethanol, and IPA. After cleaning, the substrate was exposed to UV ozone for 15 min to remove residual organic contaminants. For the hole injection layer (HIL), poly(3,4-ethylene dioxythiophene) poly(styrene sulfonate) (PEDOT:PSS, Clevios) was coated onto the substrate at 3000 rpm (37.5 nm) for 30 s and baked at 120 °C for 5 min. Then, the substrate was moved into an N_2-filled glove box (MOTEK) and was baked at 210 °C for 10 min. Subsequently, 8 mg of poly[9,9-dioctylfluorenyl-2,7-diyl]-co-(4,40-(N-(4-s-butyl phenyl)-diphenylamine)) (TFB) was used as the HTL material, which was dissolved in 1 mL of m-xylene. The solution was spin-coated at 3000 rpm (30 nm) for 30 s and then baked at 180 °C for 30 min. The InP-based QDs (25 mg/ml) were deposited at 2000 rpm (20 nm) for 30 s and were baked at 180 °C for 30 min. To obtain the QD patterns, the ALD and lithography processes were carried out. Each process is described in the *QD film patterning* section of Methods. After the lithography process, the ZnO nanoparticles (25 mg/ml) were spin-coated as an ETL at 3000 rpm (20 nm) for 30 s and baked at 110 °C for 30 min. Subsequently, Al was deposited using a thermal evaporator to prepare the cathode. The final thickness of the Al cathode was approximately 100 nm. Finally, the substrate was encapsulated using Norland Optical Adhesive (NOA) 8610 B epoxy and a coverslip for QD-LED performance.

Characterization and Analysis. PL spectra were obtained using an FC2-LED (Prizmatix) and time-resolved PL, and the absolute PLQY was obtained using a Horiba FluoroMAX Plus-C spectrofluorometer. Images of the InP-based QD patterns were obtained using a fluorescence microscope (Olympus BX51 equipped with a DP74 camera). The device performance (brightness and current density) was measured using a CS-2000 (Konica Minolta) and Keithley 2400 B. The thicknesses of the QD patterns were determined using a NanoView 3D surface profiler (NV-1800).

■ ASSOCIATED CONTENT

Supporting Information

The Supporting Information is available free of charge at https://pubs.acs.org/doi/10.1021/acsphotonics.3c00332.

PL quenching test by PAC- and PAG-based photoresists, normalized PL intensities of InP- and Cd-based QD films during each lithography step, PL intensities of blue-emitting ZnTe/ZnSe QD films during the lithography process, and schematic of the multicolor patterning process (PDF)

■ AUTHOR INFORMATION

Corresponding Author

Seong-Yong Cho − *Department of Photonics and Nanoelectronics, Hanyang University ERICA, Ansan 15588, Korea;* orcid.org/0000-0001-6948-171X; Email: seongyongcho@hanyang.ac.kr

Authors

Joon Yup Lee − *Department of Materials Science and Engineering and Department of Semiconductor Engineering, Myongji University, Yongin 17058, Korea; Department of Photonics and Nanoelectronics, Hanyang University ERICA, Ansan 15588, Korea*

Eun A Kim − *Department of Materials Science and Engineering, Myongji University, Yongin 17058, Korea; Department of Photonics and Nanoelectronics, Hanyang University ERICA, Ansan 15588, Korea*

Yeongho Choi − *Department of Energy Science and Center for Artificial Atoms, Sungkyunkwan University (SKKU), Suwon 16419, Korea*

Jisu Han − *Department of Energy Science, Center for Artificial Atoms, SKKU Institute of Energy Science and Technology (SIEST), Sungkyunkwan University (SKKU), Suwon, Gyeonggi-do 16419, Republic of Korea*

Donghyo Hahm − *SKKU Advanced Institute of Nanotechnology (SAINT), School of Nano Science & Technology, Sungkyunkwan University (SKKU), Suwon 16419, Korea*

Doyoon Shin − *SKKU Advanced Institute of Nanotechnology (SAINT), School of Nano Science & Technology, Sungkyunkwan University (SKKU), Suwon 16419, Korea*

Wan Ki Bae − *SKKU Advanced Institute of Nanotechnology (SAINT), School of Nano Science & Technology, Sungkyunkwan University (SKKU), Suwon 16419, Korea;* orcid.org/0000-0002-3832-2449

Jaehoon Lim − *Department of Energy Science, Center for Artificial Atoms, SKKU Institute of Energy Science and Technology (SIEST), Sungkyunkwan University (SKKU), Suwon, Gyeonggi-do 16419, Republic of Korea;* orcid.org/0000-0003-2623-3550

Complete contact information is available at: https://pubs.acs.org/10.1021/acsphotonics.3c00332

Notes

The authors declare no competing financial interest.

■ ACKNOWLEDGMENTS

This study was supported by the National Research Foundation (NRF) grant funded by the Korean Government (MSIT) (Grant No. NRF-2022R1A4A3018802, NRF-2021M3H4A3A01062964, and NRF-2021R1F1A1047892). J.Y.L. was also supported by the Korea Institute for Advanced Technology (KIAT) grant funded by the Korean Government (MOTIE). (P0008458, The Competency Development Program for Specialists.)

■ REFERENCES

(1) Shirasaki, Y.; Supran, G. J.; Bawendi, M. G.; Bulović, V. Emergence of Colloidal Quantum-Dot Light-Emitting Technologies. *Nat. Photonics* **2013**, *7*, 13.

(2) Jiang, Y.; Cho, S.-Y. Y.; Shim, M. Light-Emitting Diodes of Colloidal Quantum Dots and Nanorod Heterostructures for Future Emissive Displays. *J. Mater. Chem. C* **2018**, *6*, 2618−2634.

(3) Pietryga, J. M.; Park, Y.-S.; Lim, J.; Fidler, A. F.; Bae, W. K.; Brovelli, S.; Klimov, V. I. Spectroscopic and Device Aspects of Nanocrystal Quantum Dots. *Chem. Rev.* **2016**, *116*, 10513−10622.

(4) Qian, L.; Zheng, Y.; Xue, J.; Holloway, P. H. Stable and Efficient Quantum-Dot Light-Emitting Diodes Based on Solution-Processed Multilayer Structures. *Nat. Photonics* **2011**, *5*, 543−548.

(5) Dai, X.; Zhang, Z.; Jin, Y.; Niu, Y.; Cao, H.; Liang, X.; Chen, L.; Wang, J.; Peng, X. Solution-Processed, High-Performance Light-Emitting Diodes Based on Quantum Dots. *Nature* **2014**, *515*, 96−99.

(6) Dabbousi, B. O.; Bawendi, M. G.; Onitsuka, O.; Rubner, M. F. Electroluminescence from CdSe Quantum-dot/Polymer Composites. *Appl. Phys. Lett.* **1995**, *66*, 1316−1318.

(7) Colvin, V. L.; Schlamp, M. C.; Alivisatos, A. P. Light-Emitting Diodes Made from Cadmium Selenide Nanocrystals and a Semiconducting Polymer. *Nature* **1994**, *370*, 354−357.
(8) Oh, N.; Kim, B. H.; Cho, S. Y.; Nam, S.; Rogers, S. P.; Jiang, Y.; Flanagan, J. C.; Zhai, Y.; Kim, J. H.; Lee, J.; Yu, Y.; Cho, Y. K.; Hur, G.; Zhang, J.; Trefonas, P.; Rogers, J. A.; Shim, M. Double-Heterojunction Nanorod Light-Responsive LEDs for Display Applications. *Science* **2017**, *355*, 616−619.
(9) Cho, S.-Y.; Oh, N.; Nam, S.; Jiang, Y.; Shim, M. Enhanced Device Lifetime of Double-Heterojunction Nanorod Light-Emitting Diodes. *Nanoscale* **2017**, *9*, 6103−6110.
(10) Kwak, J.; Bae, W. K.; Lee, D.; Park, I.; Lim, J.; Park, M.; Cho, H.; Woo, H.; Yoon, D. Y.; Char, K.; Lee, S.; Lee, C. Bright and Efficient Full-Color Colloidal Quantum Dot Light-Emitting Diodes Using an Inverted Device Structure. *Nano Lett.* **2012**, *12*, 2362−2366.
(11) Micic, O. I.; Curtis, C. J.; Jones, K. M.; Sprague, J. R.; Nozik, A. J. Synthesis and Characterization of InP Quantum Dots. *J. Phys. Chem. A* **1994**, *98*, 4966−4969.
(12) Hahm, D.; Chang, J. H.; Jeong, B. G.; Park, P.; Kim, J.; Lee, S.; Choi, J.; Kim, W. D.; Rhee, S.; Lim, J.; Lee, D. C.; Lee, C.; Char, K.; Bae, W. K. Design Principle for Bright, Robust, and Color-Pure InP/ZnSexS1−x/ZnS Heterostructures. *Chem. Mater.* **2019**, *31*, 3476−3484.
(13) Won, Y.-H.; Cho, O.; Kim, T.; Chung, D.-Y.; Kim, T.; Chung, H.; Jang, H.; Lee, J.; Kim, D.; Jang, E. Highly Efficient and Stable InP/ZnSe/ZnS Quantum Dot Light-Emitting Diodes. *Nature* **2019**, *575*, 634−638.
(14) Han, M. G.; Lee, Y.; Kwon, H.; Lee, H.; Kim, T.; Won, Y.-H.; Jang, E. InP-Based Quantum Dot Light-Emitting Diode with a Blended Emissive Layer. *ACS Energy Lett.* **2021**, *6*, 1577−1585.
(15) Kim, T.; Kim, K.-H.; Kim, S.; Choi, S.-M.; Jang, H.; Seo, H.-K.; Lee, H.; Chung, D.-Y.; Jang, E. Efficient and Stable Blue Quantum Dot Light-Emitting Diode. *Nature* **2020**, *586*, 385−389.
(16) Lee, S.-H.; Han, C.-Y.; Song, S.-W.; Jo, D.-Y.; Jo, J.-H.; Yoon, S.-Y.; Kim, H.-M.; Hong, S.; Hwang, J. Y.; Yang, H. ZnSeTe Quantum Dots as an Alternative to InP and Their High-Efficiency Electroluminescence. *Chem. Mater.* **2020**, *32*, 5768−5775.
(17) Jang, E.; Jun, S.; Jang, H.; Lim, J.; Kim, B.; Kim, Y. White-Light-Emitting Diodes with Quantum Dot Color Converters for Display Backlights. *Adv. Mater.* **2010**, *22*, 3076−3080.
(18) Wood, V.; Panzer, M. J.; Chen, J.; Bradley, M. S.; Halpert, J. E.; Bawendi, M. G.; Bulović, V. Inkjet-Printed Quantum Dot−Polymer Composites for Full-Color AC-Driven Displays. *Adv. Mater.* **2009**, *21*, 2151−2155.
(19) Liu, Y.; Li, F.; Xu, Z.; Zheng, C.; Guo, T.; Xie, X.; Qian, L.; Fu, D.; Yan, X. Efficient All-Solution Processed Quantum Dot Light Emitting Diodes Based on Inkjet Printing Technique. *ACS Appl. Mater. Interfaces* **2017**, *9*, 25506−25512.
(20) Roh, H.; Ko, D.; Shin, D. Y.; Chang, J. H.; Hahm, D.; Bae, W. K.; Lee, C.; Kim, J. Y.; Kwak, J. Enhanced Performance of Pixelated Quantum Dot Light-Emitting Diodes by Inkjet Printing of Quantum Dot−Polymer Composites. *Adv. Opt. Mater.* **2021**, *9*, No. 2002129.
(21) Kim, T.-H.; Cho, K.-S.; Lee, E. K.; Lee, S. J.; Chae, J.; Kim, J. W.; Kim, D. H.; Kwon, J.-Y.; Amaratunga, G.; Lee, S. Y.; Choi, B. L.; Kuk, Y.; Kim, J. M.; Kim, K. Full-Colour Quantum Dot Displays Fabricated by Transfer Printing. *Nat. Photonics* **2011**, *5*, 176−182.
(22) Kim, B. H.; Nam, S.; Oh, N.; Cho, S.-Y.; Yu, K. J.; Lee, C. H.; Zhang, J.; Deshpande, K.; Trefonas, P.; Kim, J.-H.; Lee, J.; Shin, J. H.; Yu, Y.; Lim, J.; bin Won, S. M.; Cho, Y. K.; Kim, N. H.; Seo, K. J.; Lee, H.; Kim, T.; Shim, M.; Rogers, J. A. Multilayer Transfer Printing for Pixelated, Multicolor Quantum Dot Light-Emitting Diodes. *ACS Nano* **2016**, *10*, 4920−4925.
(23) Choi, M. K.; Yang, J.; Kang, K.; Kim, D. C.; Choi, C.; Park, C.; Kim, S. J.; Chae, S. I.; Kim, T.-H.; Kim, J. H.; Hyeon, T.; Kim, D.-H. Wearable Red−Green−Blue Quantum Dot Light-Emitting Diode Array Using High-Resolution Intaglio Transfer Printing. *Nat. Commun.* **2015**, *6*, No. 7149.
(24) Kim, T.-H.; Chung, D.-Y.; Ku, J.; Song, I.; Sul, S.; Kim, D.-H.; Cho, K.-S.; Choi, B. L.; Min Kim, J.; Hwang, S.; Kim, K. Heterogeneous Stacking of Nanodot Monolayers by Dry Pick-and-Place Transfer and Its Applications in Quantum Dot Light-Emitting Diodes. *Nat. Commun.* **2013**, *4*, No. 2637.
(25) Cho, H.; Pan, J.-A.; Wu, H.; Lan, X.; Coropceanu, I.; Wang, Y.; Cho, W.; Hill, E. A.; Anderson, J. S.; Talapin, Dv. Direct Optical Patterning of Quantum Dot Light-Emitting Diodes via In Situ Ligand Exchange. *Adv. Mater.* **2020**, *32*, No. 2003805.
(26) Yang, J.; Hahm, D.; Kim, K.; Rhee, S.; Lee, M.; Kim, S.; Chang, J. H.; Park, H. W.; Lim, J.; Lee, M.; Kim, H.; Bang, J.; Ahn, H.; Cho, J. H.; Kwak, J.; Kim, B.; Lee, C.; Bae, W. K.; Kang, M. S. High-Resolution Patterning of Colloidal Quantum Dots via Non-Destructive, Light-Driven Ligand Crosslinking. *Nat. Commun.* **2020**, *11*, No. 2874.
(27) Kim, G.-H.; Lee, J.; Lee, J. Y.; Han, J.; Choi, Y.; Kang, C. J.; Kim, K.-B.; Lee, W.; Lim, J.; Cho, S.-Y. High-Resolution Colloidal Quantum Dot Film Photolithography via Atomic Layer Deposition of ZnO. *ACS Appl. Mater. Interfaces* **2021**, *13*, 43075−43084.
(28) Ko, J.; Chang, J. H.; Jeong, B. G.; Kim, H. J.; Joung, J. F.; Park, S.; Choi, D. H.; Bae, W. K.; Bang, J. Direct Photolithographic Patterning of Colloidal Quantum Dots Enabled by UV-Crosslinkable and Hole-Transporting Polymer Ligands. *ACS Appl. Mater. Interfaces* **2020**, *12*, 42153−42160.
(29) Lee, J. Y.; Kim, E. A.; Han, J.; Choi, Y.-H.; Hahm, D.; Kang, C. J.; Bae, W. K.; Lim, J.; Cho, S.-Y. Nondestructive Direct Photolithography for Patterning Quantum Dot Films by Atomic Layer Deposition of ZnO. *Adv. Mater. Interfaces* **2022**, *9*, No. 2200835.
(30) Yang, J.; Lee, M.; Park, S. Y.; Park, M.; Kim, J.; Sitapure, N.; Hahm, D.; Rhee, S.; Lee, D.; Jo, H.; Jo, Y. H.; Lim, J.; Kim, J.; Shin, T. J.; Lee, D. C.; Kwak, K.; Kwon, J. S.; Kim, B.; Bae, W. K.; Kang, M. S. Nondestructive Photopatterning of Heavy-Metal-Free Quantum Dots. *Adv. Mater.* **2022**, *34*, No. 2205504.
(31) Hahm, D.; Lim, J.; Kim, H.; Shin, J.-W.; Hwang, S.; Rhee, S.; Chang, J. H.; Yang, J.; Lim, C. H.; Jo, H.; Choi, B.; Cho, N. S.; Park, Y.-S.; Lee, D. C.; Hwang, E.; Chung, S.; Kang, C.; Kang, M. S.; Bae, W. K. Direct Patterning of Colloidal Quantum Dots with Adaptable Dual-Ligand Surface. *Nat. Nanotechnol.* **2022**, *17*, 952−958.
(32) Li, F.; Chen, C.; Lu, S.; Chen, X.; Liu, W.; Weng, K.; Fu, Z.; Liu, D.; Zhang, L.; Abudukeremu, H.; Lin, L.; Wang, Y.; Zhong, M.; Zhang, H.; Li, J. Direct Patterning of Colloidal Nanocrystals via Thermally Activated Ligand Chemistry. *ACS Nano* **2022**, *16*, 13674−13683.
(33) Yun, H.-S.; Noh, K.; Kim, J.; Noh, S. H.; Kim, G.-H.; Lee, W.; Na, H.; Bin; Yoon, T.-S.; Jang, J.; Kim, Y.; Cho, S.-Y. CsPbBr3 Perovskite Quantum Dot Light-Emitting Diodes Using Atomic Layer Deposited Al2O3 and ZnO Interlayers. *Phys. Status Solidi RRL* **2020**, *14*, No. 2070012.
(34) Kim, G.-H.; Noh, K.; Han, J.; Kim, M.; Oh, N.; Lee, W.; Na, H. bin.; Shin, C.; Yoon, T.-S.; Lim, J.; Cho, S.-Y. Enhanced Brightness and Device Lifetime of Quantum Dot Light-Emitting Diodes by Atomic Layer Deposition. *Adv. Mater. Interfaces* **2020**, *7*, No. 2000343.
(35) Gao, H.; Qie, Y.; Zhao, H.; Li, F.; Guo, T.; Hu, H. High-Performance, High-Resolution Quantum Dot Light-Emitting Devices through Photolithographic Patterning. *Org. Electron* **2022**, *108*, No. 106609.
(36) Jeong, B. G.; Chang, J. H.; Hahm, D.; Rhee, S.; Park, M.; Lee, S.; Kim, Y.; Shin, D.; Park, J. W.; Lee, C.; Lee, D. C.; Park, K.; Hwang, E.; Bae, W. K. Interface Polarization in Heterovalent Core−Shell Nanocrystals. *Nat. Mater.* **2022**, *21*, 246−252.
(37) Borg, L. z.; Lee, D.; Lim, J.; Bae, W. K.; Park, M.; Lee, S.; Lee, C.; Char, K.; Zentel, R. The Effect of Band Gap Alignment on the Hole Transport from Semiconducting Block Copolymers to Quantum Dots. *J. Mater. Chem. C* **2013**, *1*, 1722−1726.
(38) Bae, W. K.; Nam, M. K.; Char, K.; Lee, S. Gram-Scale One-Pot Synthesis of Highly Luminescent Blue Emitting Cd1−xZnxS/ZnS Nanocrystals. *Chem. Mater.* **2008**, *20*, 5307−5313.
(39) Janssen, R. A. J.; Stouwdam, J. W. Red, Green, and Blue Quantum Dot LEDs with Solution Processable ZnO Nanocrystal Electron Injection Layers. *J. Mater. Chem.* **2008**, *18*, 1889−1894.

https://doi.org/10.1021/acsphotonics.3c00332
ACS Photonics 2023, 10, 2598−2607

(40) Noh, K.; Kim, M.; Lee, S. H.; Yun, H. S.; Lim, T. H.; Choi, Y.; Kim, K. J. B.; Jiang, Y.; Beom, K.; Kim, M.; Kim, Y. G.; Lee, P.; Oh, N.; Kim, B. H.; Shin, C.; Lee, H. H.; Yoon, T.-S.; Shim, M.; Lim, J.; Kim, K.-B.; Cho, S. Y. Effect of Ethanolamine Passivation of ZnO Nanoparticles in Quantum Dot Light Emitting Diode Structure. *Curr. Appl. Phys.* **2019**, *19*, 998−1005.

https://doi.org/10.1021/acsphotonics.3c00332
ACS Photonics 2023, 10, 2598−2607